

# AIF depletion provides neuroprotection through a preconditioning effect

Eva-Maria Öxler · Amalia Dolga · C. Culmsee

Published online: 4 August 2012  
© Springer Science+Business Media, LLC 2012

**Abstract** Previous studies established a major role for apoptosis inducing factor (AIF) in neuronal cell death after acute brain injury. For example, AIF translocation from mitochondria to the nucleus determined delayed neuronal death, whereas reduced AIF expression provided neuroprotective effects in models of cerebral ischemia or brain trauma. The question remains, however, why reduced AIF levels are sufficient to mediate neuroprotection, since only very little AIF translocation to the nucleus is required for induction of cell death. Thus, the present study addresses the question, whether AIF gene silencing affects intrinsic death pathways upstream of nuclear translocation at the level of the mitochondria. Using MTT assays and real-time cell impedance measurements we confirmed the protective effect of AIF siRNA against glutamate toxicity in immortalized mouse hippocampal HT-22 neurons. Further, AIF siRNA prevented glutamate-induced mitochondrial fragmentation and loss of mitochondrial membrane potential. The protection of mitochondrial integrity was associated with preserved ATP levels, attenuated increases in lipid peroxidation and reduced complex I expression levels. Notably, low concentrations of the complex I inhibitor rotenone (20 nM), provided similar protective effects against glutamate toxicity at the mitochondrial level. These results expose a preconditioning effect as a

mechanism for neuroprotection mediated by AIF depletion. In particular, they point out an association between mitochondrial complex I and AIF, which regulate each other's stability in mitochondria. Overall, these findings postulate that AIF depletion mediates a preconditioning effect protecting neuronal cells from subsequent glutamate toxicity through reduced levels of complex I protein.

**Keywords** AIF · Rotenone · Preconditioning · Complex I · Mitochondria · Neuroprotection

## Abbreviations

ANOVA	Analysis of variance
AIF	Apoptosis inducing factor
BODIPY	4,4-Difluoro-5-(4-phenyl-1,3-butadienyl)-4-bora-3a,4a-diaza-sindacene-3-undecanoic acid
DMEM	Dulbecco's Modified Eagle Medium
DMSO	Dimethylsulfoxide
DTT	DL-Dithiothreitol
EDTA	Ethylenediaminetetraacetic acid
EGTA	Ethylene glycol-bis(2-aminoethylether)-N,N,N',N'-tetraacetic acid
ES	Embryonic stem
FACS	Fluorescence-activated cell sorting
HEPES	4-(2-Hydroxyethyl)piperazine-1-ethanesulfonic acid
Hq	Harlequin
mPTP	Mitochondrial permeability transition pore
MMP	Mitochondrial membrane potential
MTT	3-(4,5-Dimethylthiazol-2-yl)-2,5-diphenyltetrazolium bromide
PARP-1	Poly(ADP-ribose)polymerase 1
PBS	Phosphate buffered solution
TMRE	Tetramethylrhodamin ethyl ester

E.-M. Öxler · A. Dolga · C. Culmsee (✉)  
Fachbereich Pharmazie, Institut für Pharmakologie  
und Klinische Pharmazie, Philipps-Universität Marburg,  
Karl-von-Frisch-Straße 1, 35032 Marburg, Germany  
e-mail: culmsee@staff.uni-marburg.de

E.-M. Öxler  
e-mail: oexlere@staff.uni-marburg.de

A. Dolga  
e-mail: dolga@staff.uni-marburg.de

## Introduction

Apoptosis inducing factor (AIF) is a nuclear encoded ~62 kDa flavoprotein that is located in the inner mitochondrial membrane from where it is released and translocated to the nucleus during cell death. In fact, AIF was the first mitochondrial protein shown to mediate caspase-independent cell death [1, 2]. During intrinsic cell death AIF is cleaved into a ~57 kDa form that is released from the mitochondria and translocates to the nucleus where it induces chromatin condensation and large-scale DNA fragmentation [1, 2]. It is now well established that AIF-dependent cell death plays a key role in neuronal death after acute brain damage in model systems of cerebral ischemia [3–5], traumatic brain injury [6] or epileptic seizures [7]. The cumulative evidence for a key role of AIF translocation to the nucleus in paradigms of cell death led to the conclusion that controlling AIF upstream of mitochondrial release may emerge as a promising therapeutic strategy in neurological diseases, such as cerebral ischemia or neurodegenerative disorders [8]. Direct inhibition of AIF by small molecules is not available so far and previous neuroprotective effects were achieved using siRNA-mediated gene silencing or in genetic models of reduced AIF expression, such as harlequin (Hq) mice, which express only 20 % AIF compared to wildtype mice [5, 9].

Despite the cumulative evidence for neuroprotective effects obtained by reduced AIF expression levels *in vitro* and *in vivo*, the exact mechanism by which AIF depletion sustains neuronal survival remains unknown. In particular, it is controversial that AIF depletion mediates neuroprotection just because of reduced translocation of the protein to the nucleus, since neurons of Hq mice or after AIF siRNA treatment still express considerable amounts of AIF, which would be sufficient for nuclear translocation and induction of cell death after mitochondrial release. In fact, very little amounts of cytosolic AIF are sufficient for translocation to the nucleus, detrimental DNA fragmentation and induction of cell death. Moreover, the fast kinetics of AIF release to the nucleus [10] disagrees with a direct protective effect by just reduced AIF levels. Thus, other effects may be responsible for the neuroprotective effect of AIF deficiency for example, metabolic effects. Since AIF is a flavoprotein containing binding sites for FAD and NADH with putative NADH and NADPH oxidase activities [11], loss of AIF may affect the redox balance in mitochondria. In fact, previous studies have shown that AIF-depleted cells like AIF<sup>-/-</sup> ES (embryonic stem) and Hq cells exert defects in oxidative phosphorylation and mitochondrial respiratory complex stability [12, 13]. These findings point at the metabolic impact of AIF deficiencies, which may play an important role for the integrity, structure and function of the mitochondria, including the activity and

stability of the respiratory chain [14, 15]. Notably, inhibition of the mitochondrial respiratory chain can provide preconditioning effects protecting cells from a following lethal stress [16].

The aim of the current study was to investigate whether AIF depletion mediates mitochondrial preconditioning in a model system of glutamate toxicity in immortalized hippocampal HT-22 neurons where glutamate induces lethal oxidative stress, mitochondrial fragmentation and intrinsic pathways of AIF-dependent cell death [17–19]. The effects of AIF siRNA in the model system of glutamate-induced oxytosis were compared to rotenone, a specific mitochondrial complex I inhibitor. Our results support the hypothesis that AIF depletion mediates a preconditioning effect at the level of mitochondria thereby mediating protection of neuronal cells from subsequent glutamate toxicity.

## Results

### AIF gene silencing by siRNA attenuates glutamate neurotoxicity

Downregulation of AIF was achieved using two different sequences of AIF-targeting siRNA (AIF siRNA 1 and AIF siRNA 2). Both sequences specifically reduced AIF expression as shown by RT-PCR and Western Blot analysis (Fig. 1a). The AIF siRNAs significantly attenuated glutamate-induced cell death. HT-22 neurons exposed to glutamate for 11–15 h showed typical morphology of cell death: the neuronal cells appear rounded, shrunken and detached from the culture dish whereas AIF-silenced cells preserved their normal spindle-shaped morphology and were rescued from glutamate-induced apoptosis (Fig. 1b). Cell viability was quantified using the MTT assay, which confirmed the protective effect of the AIF siRNAs (Fig. 2a, b). Further, real-time detection of cell death was performed by impedance measurements over at least 15 h with the xCELLigence system, which revealed delayed cell death in AIF-depleted cells. Best protective effects were achieved with transfection of AIF siRNA 2, which showed sustained protection against cell death and proliferation over time similar to cells transfected with scrambled (scr) siRNA. In contrast, AIF siRNA 1 only provided transient protective effects with a delay of cell death of 1–2 h compared to controls exposed to glutamate (Fig. 2c, d).

### AIF siRNA preserves mitochondrial integrity

In order to investigate if the protective effect of AIF deficiency was attributed to a preconditioning effect at the level of mitochondria, we next examined mitochondrial morphology and function. Neurons exposed to glutamate

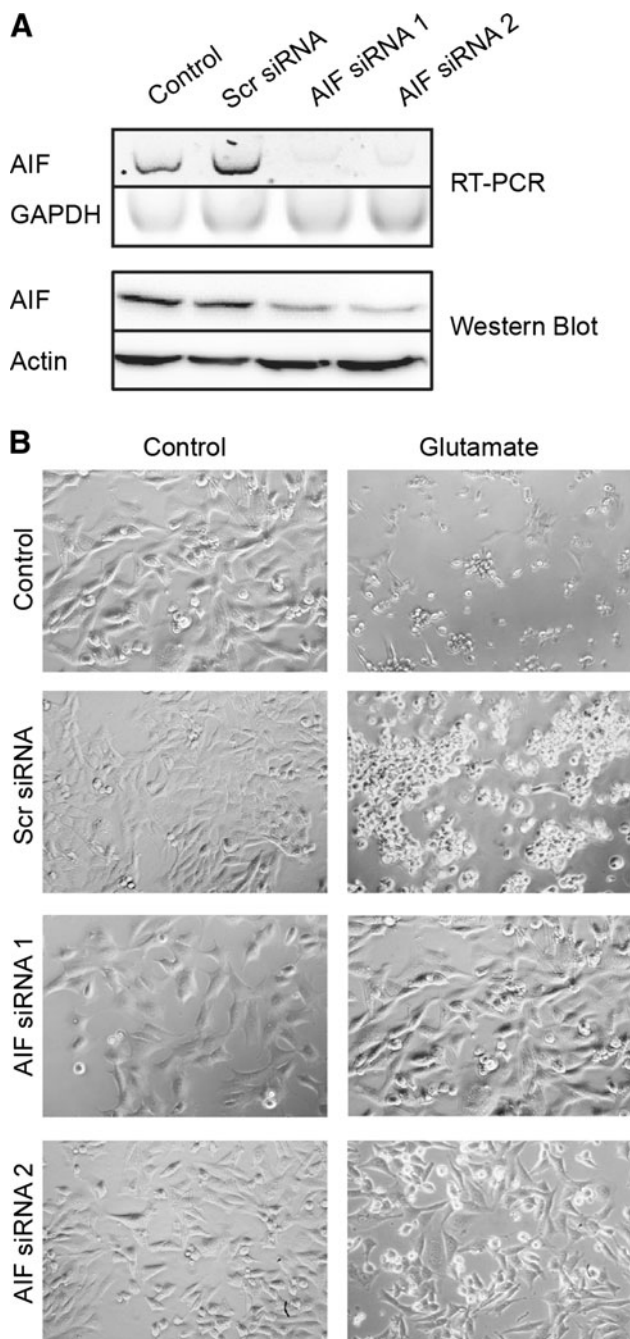


**Fig. 1** AIF knockdown by different AIFsiRNA sequences attenuates glutamate toxicity. **a** AIF knockdown was verified by RT-PCR and Western Blot analysis 72 h after transfection. AIF expression of AIF siRNA transfected cells was compared to non-transfected control cells and cells treated with *scr* siRNA. **b** AIF siRNA (20 nM) preserves the phenotype from glutamate-induced (5 mM, 12 h) apoptosis compared to non-transfected control cells and cells transfected with *scr* siRNA ( $\times 10$ )

toxicity show disturbed mitochondrial morphology dynamics resulting in detrimental mitochondrial fragmentation [18, 19]. The increased rate of mitochondrial fission in damaged HT-22 cells as well as peri-nuclear accumulation of

the organelles was prevented by AIF siRNA 1 and 2 (Fig. 3a, b). This suggested that the protective mechanism underlying AIF deficiency occurred before the release of AIF from the mitochondria into the cytosol.

To prove this conclusion we next analyzed the formation of lipid peroxides, which are associated with irreversible mitochondrial damage and reactive oxygen species (ROS) formation. AIF silencing significantly reduced the production of lipid peroxides compared to controls exposed to glutamate (Fig. 4a). Again, AIF siRNA 2 mediated stronger protective effects compared to AIF siRNA 1 especially at later time points of glutamate treatment. For that reason AIF siRNA 2 was used for further investigations.

To assess the functional integrity of mitochondria in AIF-depleted cells we next examined ATP levels after glutamate exposure. Since cell injury results in a rapid decrease in cytoplasmic ATP levels we wanted to test if the AIF-depleted cells showed alterations in ATP levels in the absence or presence of toxic glutamate concentrations. In both cases, ATP levels of transfected cells were similar to the ATP levels in non-treated control cells (Fig. 4b). The endpoint for the experiment was assessed for the glutamate-treated cells starting with the onset of cell morphology alteration and culminating with the cell detachment and death [20, 21].

To further test for functional integrity we investigated the mitochondrial membrane potential (MMP) in controls compared to AIF-silenced cells. Under standard culture conditions, AIF-depleted cells showed significantly lower MMP than in control cells as detected by TMRE and DIOC6(3) staining and associated analysis (Fig. 5a, b). Further, TMRE staining revealed that glutamate toxicity was associated with pronounced mitochondrial membrane depolarization as detected in non-treated cells and cells treated with *scr* non-silencing siRNA whereas AIF-depleted cells showed significantly higher MMP at the same time point.

#### Silencing of AIF mediates decreases in mitochondrial complex I expression

Experiments in different cell models implied that AIF deficiency leads to reduced levels of mitochondrial complex I. Thus, we determined the mitochondrial complex protein expression by Western Blot in AIF-silenced HT-22 cells. AIF-depleted cells showed significantly reduced levels of complex I 72 h after transfection (Fig. 6a, b). Other complexes of the respiratory chain were not affected by AIF siRNA in these cells. Interestingly, treatment with the specific complex I inhibitor rotenone was also associated with slightly decreased expression levels of AIF. This suggests that mitochondrial complex I and AIF may regulate each other's stability in mitochondria.

**Fig. 2** AIF depletion preserves cell viability. **a** MTT assay confirms protective effect of AIF depletion by AIF siRNA 1 (20 nM) following glutamate exposure (5 mM, 11 h) ( $n = 7$ ;  $***p < 0.001$ , compared to glutamate treated control and *scr* siRNA). **b** MTT assay 72 h after transfection shows protective effect of AIF siRNA 2 (20 nM) towards glutamate exposure (3 mM, 12 h) ( $**p < 0.01$ ;  $n = 6$ , compared to glutamate treated control and *scr* siRNA). Statistics were obtained using ANOVA, Scheffé test. **c, d** xCELLigence real-time measurement: HT-22 cells were treated with glutamate (glut) 3 mM 72 h after transfection. AIF siRNA 1 (20 nM) shows short transient protective effect against glutamate-induced cell death compared to cells transfected with *scr* siRNA (**c**) ( $n = 5$ ). AIF siRNA 2 (20 nM) shows stronger protection over time (**d**) ( $n = 8$ )

Low dose rotenone treatment preserves cells from glutamate neurotoxicity

To further link the determined protective effects of AIF deficient cells with the downregulation of mitochondrial complex I we tested if inhibition of complex I by rotenone might also result in a neuroprotective effect in our model system. Using MTT assays and impedance measurements, we found neuroprotection of the complex I inhibitor rotenone by using concentrations in the nanomolar range (Fig. 7a). This protective effect was observed in a co-treatment with glutamate and rotenone (Fig. 7a) as well as in a pre-treatment with rotenone followed by a washout before the glutamate treatment (Fig. 7b). Higher concentrations of rotenone ( $>50$  nM) induced about 45 % apoptosis in HT-22 cells during the same time of treatment (data not shown). Similar to AIF-depleted cells we found just a transient protection against glutamate-induced cell death when measuring cell viability by impedance measurements in cells pre-treated with rotenone (Fig. 7b).

Notably, mitochondrial fragmentation as a sign of disturbed mitochondrial morphology dynamics was also attenuated when HT-22 neurons were treated with rotenone (Fig. 8a, b). After glutamate treatment, rotenone receiving cells showed higher amounts of long tubular mitochondria of category I compared to control cells and lower amounts of fragmented mitochondria of category III.

Further, to prove our hypothesis that slight complex I inhibition preserves from glutamate toxicity by a preconditioning effect we investigated levels of lipid peroxides after rotenone treatment. Rotenone alone did not alter lipid peroxide levels under standard culture conditions but it preserved cells from an increase in lipid peroxides and thus in ROS production after the glutamate challenge (Fig. 8c). As in AIF-depleted cells we also investigated MMP of rotenone-treated cells as a further test for functional integrity. Cells with rotenone-mediated complex I inhibition showed significantly lower MMP than control cells. These findings confirmed the conclusion that AIF-silenced cells follow a similar preconditioning effect as rotenone-treated cells, i.e. through reduced activity of mitochondrial

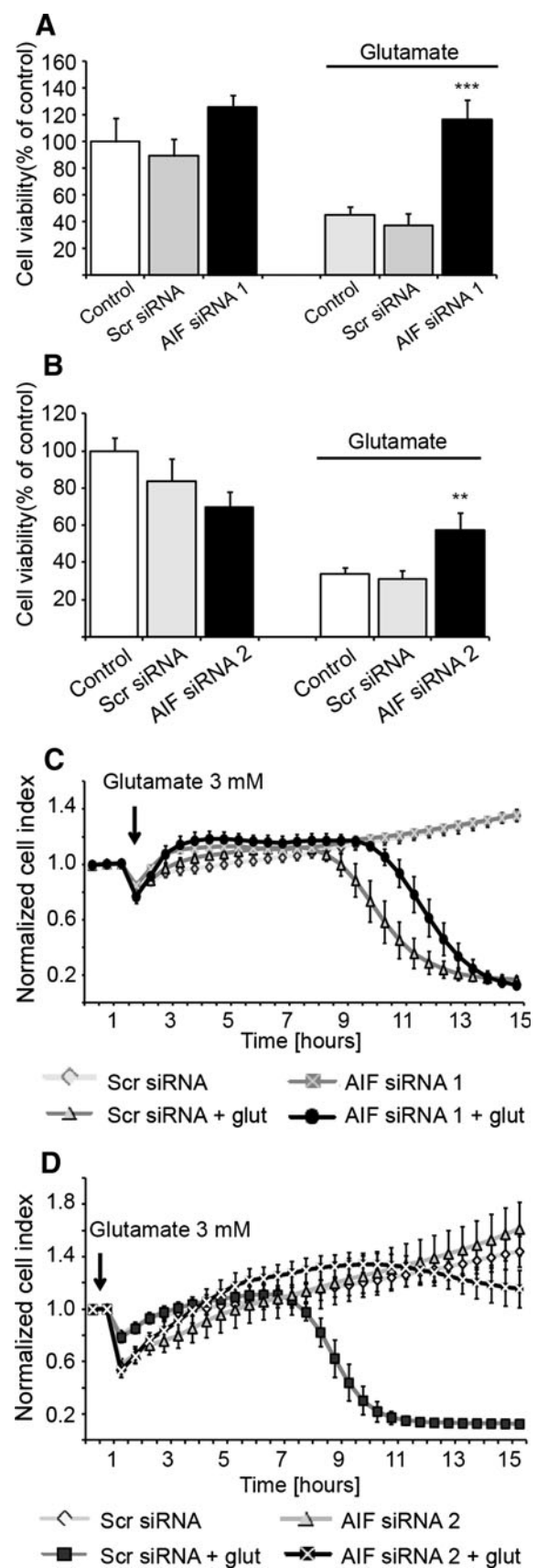


**Fig. 3** AIF siRNA preserves mitochondrial morphology. **a** Fluorescence photomicrographs show that AIF siRNA (20 nM) prevents the fission of mitochondria in glutamate-exposed (3 mM, 14 h) HT-22 cells compared to non-transfected control cells and cells transfected with *scr* siRNA. Cells were stained with Mitotracker red 30 min before glutamate treatment. Scale bar 20  $\mu$ m. **b** Quantification of mitochondrial morphology: Category I (*Cat I*): fused, Category II (*Cat II*): intermediate, Category III (*Cat III*): fragmented mitochondria; at least 500 cells were counted per condition blind to treatment conditions. Values are given from six independent experiments (<sup>###</sup> $p < 0.001$  compared to category I glutamate treated control and *scr* siRNA; <sup>\*\*\*</sup> $p < 0.001$  compared to category III glutamate treated control and scrambled (*scr*) siRNA). Statistics were obtained using ANOVA, Scheffé test

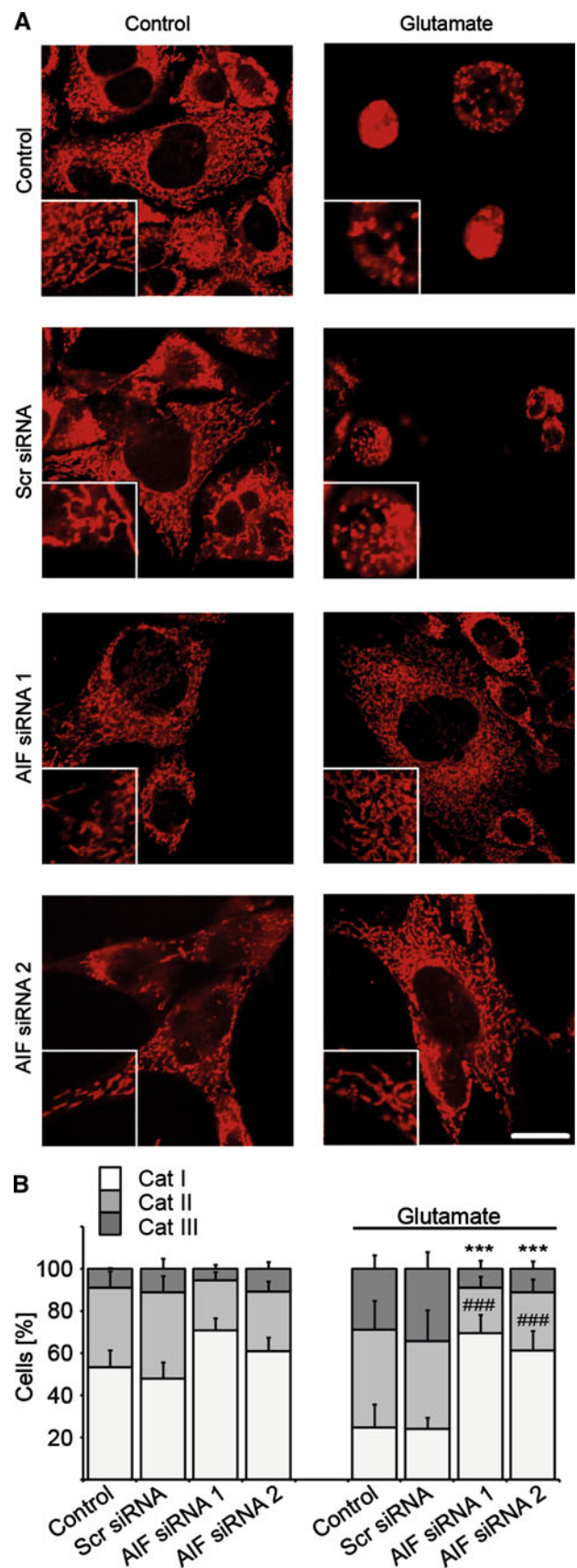
complex I. Furthermore, glutamate-induced ultimate mitochondrial depolarization as a late endpoint of the mitochondrial damage in this model system of oxytosis was prevented in rotenone-treated cells (Fig. 5b, c).

Since it is known that strong inhibition of complex I alters cytoplasmic ATP levels [9] we investigated ATP levels in HT-22 cells receiving low doses of rotenone. In a concentration of 20 nM rotenone did not affect basal levels of ATP. However glutamate-induced loss of ATP levels was prevented by rotenone in the same concentration, which further confirmed its neuroprotective effect (Fig. 8d).

## Discussion

The present study provides evidence for a preconditioning effect by AIF gene silencing, which protects mitochondrial function and integrity in a paradigm of lethal oxidative stress in a neural cell line. Depletion of AIF preserved mitochondrial morphology, MMP and ATP levels after induction of oxidative stress in HT-22 cells, and this mitoprotective effect also significantly attenuated the secondary increase in lipid peroxidation, which was associated with mitochondrial damage and cell death in this model system [22]. Preconditioning by AIF depletion was associated with reduced complex I expression levels. Low doses of the complex I inhibitor rotenone achieved protective effects against glutamate-induced cell death in our model system similar to the effects observed after AIF silencing. These results suggest that AIF silencing provides protection against oxidative cell death at the level of mitochondria and not at the level of apoptotic DNA damage in the nucleus.

AIF is a key player in mediating apoptotic nuclear changes once it is released from mitochondria [1, 2]. Over time different modulators of mitochondrial AIF release were identified such as calpain I, which can induce cleavage and release of AIF from isolated mitochondria



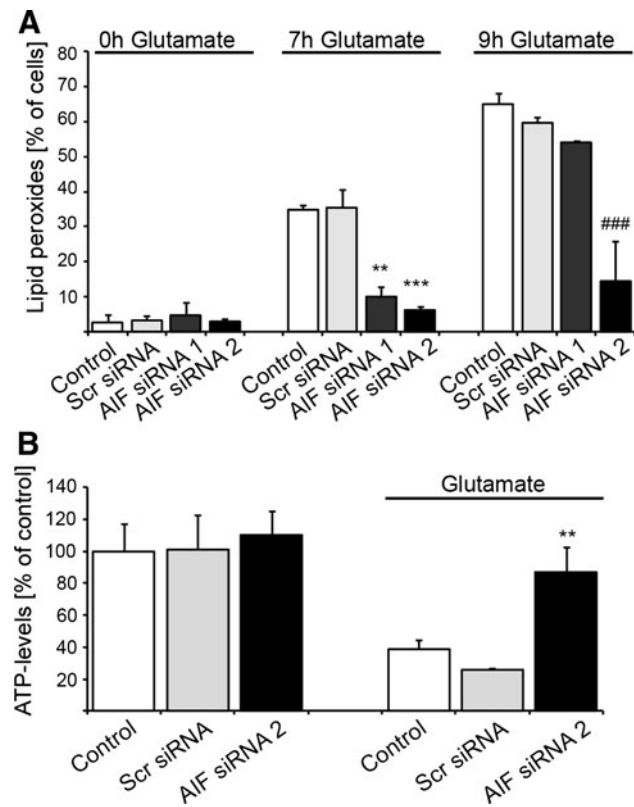


**Fig. 4** AIF siRNA preserves mitochondrial integrity. **a** Lipid peroxides were measured by Bodipy FACS analysis at different time points following glutamate treatment (5 mM). Values are given from three independent experiments; \*\* $p < 0.01$  \*\*\* $p < 0.001$  compared to glutamate treated controls and *scr* siRNA (7 h); ### $p < 0.001$  compared to glutamate treated controls and *scr* siRNA (9 h). **b** Forty-eight hours after transfection cells were seeded into 96-well plates. Following 24 h cells were treated with glutamate (3 mM) for 11 h. ATP levels from AIF siRNA transfected cells (20 nM) were preserved from loss in ATP levels ( $n = 6$ ; \*\* $p < 0.01$  compared to glutamate treated control cells and *scr* siRNA). Statistics were obtained using ANOVA, Scheffé test

[23]. Further, we demonstrated that the proapoptotic protein Bid mediated mitochondrial release of AIF in neural cells [10, 19, 20]. In addition, poly(ADP-ribose)polymerase 1 (PARP-1) activity was linked to detrimental AIF release and genetic deletion or pharmacological inhibition of PARP-1 prevented AIF translocation and protected neurons from cell death in vitro and in vivo [24–26]. While these regulators of mitochondrial damage and AIF release were validated as potential therapeutic targets in models of neuronal degeneration and death, direct inhibition of AIF by pharmacological compounds is not available so far. The only evidence for protection against neuronal death by AIF inhibition derives from experimental settings using AIF siRNA and Hq mice [3–7, 27]. These mice have a proviral insertion in the AIF gene, causing about 80 % reduction in AIF expression [28].

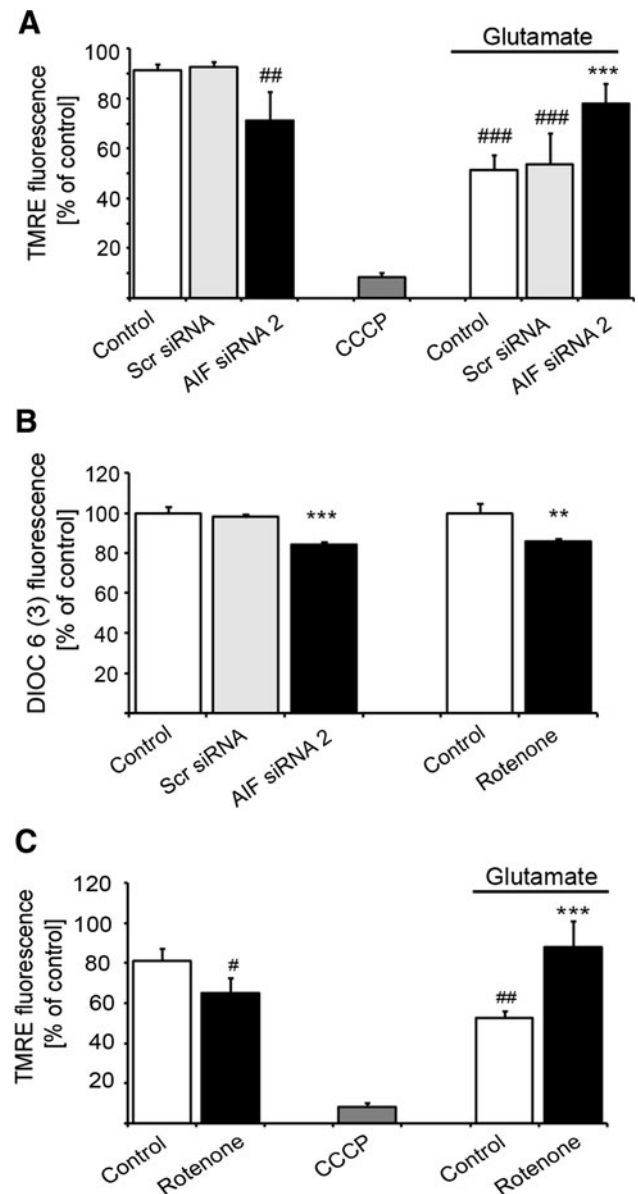


**Fig. 5** Preservation and depolarization of MMP. **a** MMP measured by TMRE is protected from glutamate excitotoxicity (3 mM, 15 h). In AIF-depleted cells MMP is significantly depolarized. Values are given from six independent experiments; ### $p < 0.001$ ; ## $p < 0.01$  compared to untreated control cells and *scr* siRNA; \*\*\* $p < 0.001$  compared to glutamate treated control cells and *scr* siRNA. **b** Seventy-two hours after transfection MMP was measured by DIOC6(3) assay. AIF-depleted mitochondria and rotenone receiving cells (20 nM, 18 h) are depolarized ( $n = 3$ ; \*\*\* $p < 0.001$ ; ## $p < 0.01$  compared to control). **c** MMP measured by TMRE is significantly ( $#p < 0.05$ ) decreased by rotenone (20 nM, 15 h) compared to control cells. After glutamate treatment (3 mM, 15 h) membrane potential is preserved by rotenone (20 nM) (\*\*\*) compared to glutamate treated control cells. Values are given from four independent experiments. All statistics were obtained using ANOVA, Scheffé test

However, the detrimental nuclear changes and DNA fragmentation occur within a few minutes after AIF release from the mitochondria [29] and very little AIF protein that

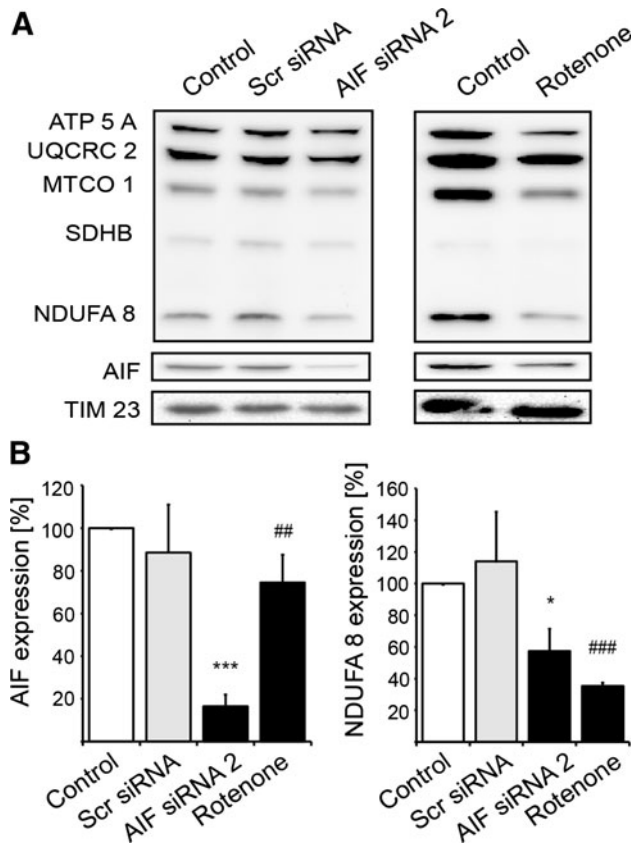


**Fig. 6** Preconditioning effect mediated by mitochondrial complex I downregulation. **a** Western Blots show that AIF depletion leads to a downregulation of complex I (NDUFA 8) 72 h after transfection. Furthermore, rotenone treatment (20 nM, 18 h) leads to a slight decrease of AIF expression. **b** Quantification of Western Blot analysis. AIF and NDUFA 8 specific bands were normalized to TIM 23. Values are given as percentage of control from four independent experiments. \*\*\* $p < 0.001$ , \* $p < 0.05$  compared to *scr* siRNA; # $p < 0.01$ , ### $p < 0.001$  compared to control (Scheffé test)

is still present after AIF siRNA treatment or in Hq mice are able to induce programmed cell death [22, 29]. For example, we showed that AIF siRNA prevented cell death in neuronal cells exposed to oxygen-glucose deprivation (OGD) or glutamate [10] and Cheung et al. [14] demonstrated sustained neuronal survival after DNA damage and excitotoxic induced cell death in Hq/*Apaf1*<sup>-/-</sup> double mutant mice. Further, AIF deficiency protected brain tissue of Hq mice against hypoxia/ischemia [5, 27], focal cerebral ischemia [3, 4] or ionizing radiation in vivo [30]. The fact that the model systems that show neuroprotection mediated by AIF depletion retain low AIF expression levels, postulates a metabolic effect to be responsible for the benefit of AIF deficiency. It is known that the major biochemical defects mediated by AIF depletion are changes in the respiratory chain complex I [13, 14]. This phenotype was shown to develop progressively in Hq mice [31].

Here, we found that the protective effect of AIF silencing was associated with reduced complex I expression levels in

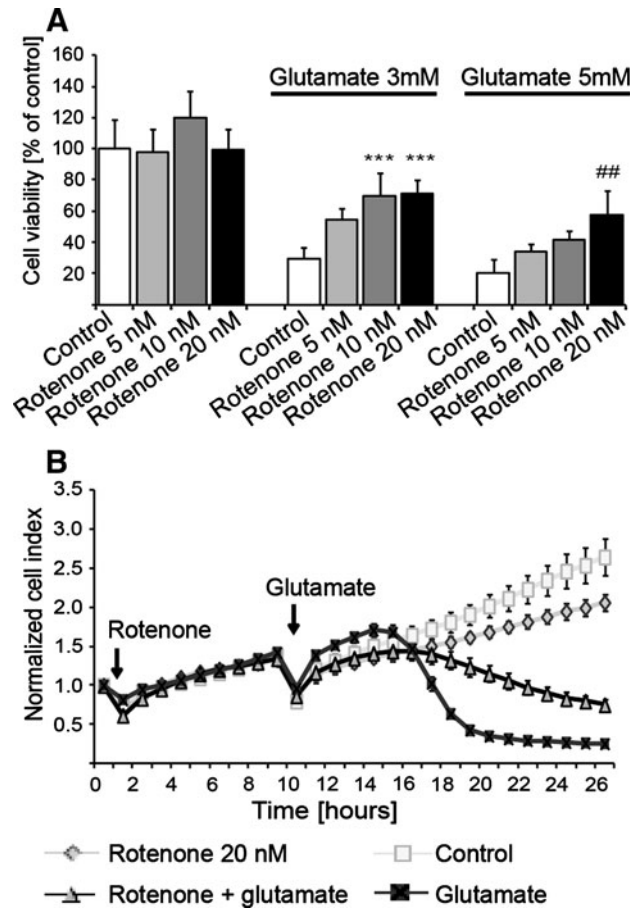


**Fig. 7** Low dose rotenone leads to transient neuroprotective effects by preconditioning. **a** MTT assays show that rotenone (10 and 20 nM) is able to protect HT-22 cells from glutamate-induced (3 and 5 mM, 13 h) cell death ( $n = 8$ ; \*\*\* $p < 0.001$  compared to glutamate treated control (3 mM); ## $p < 0.01$  compared to glutamate treated control (5 mM); ANOVA, Scheffé test). **b** HT-22 cells were plated on an E-plate 96 and cellular impedance was continuously monitored by the xCELLigence system. Cells were pre-treated with rotenone 20 nM for 9 h. After washout of rotenone pre-treated cells show a transient protective effect against glutamate-induced cell death (3 mM) ( $n = 6$ )

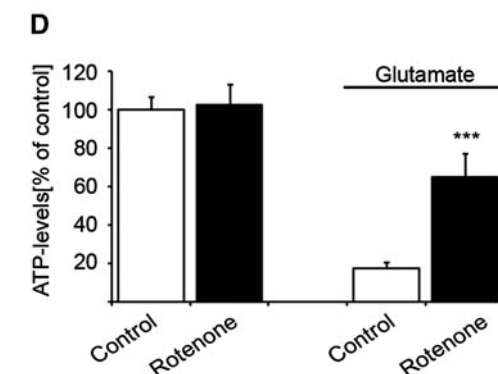
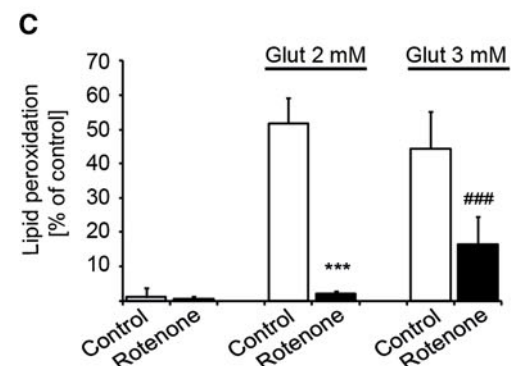
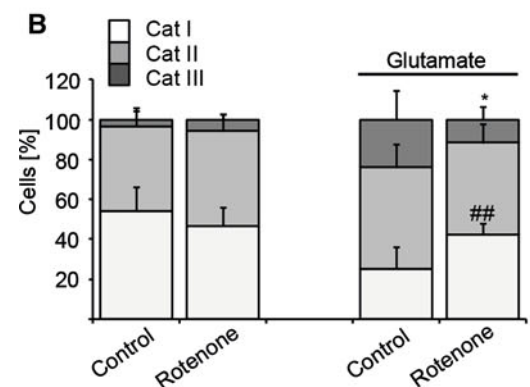
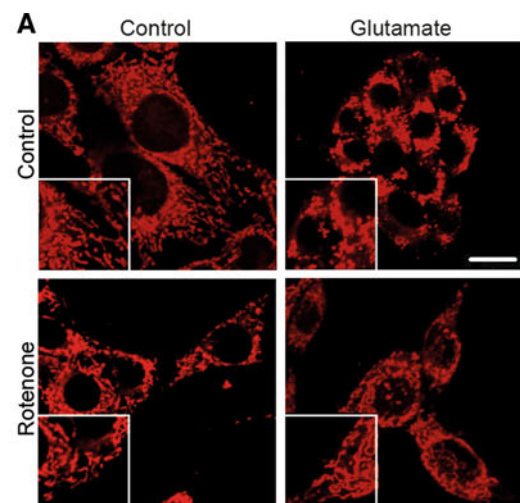
the HT-22 cells, which is consistent with previous reports in Hq mice and other cell models for AIF depletion [13, 31]. Further, direct inhibition of complex I by the inhibitor rotenone in nM range also decelerates mitochondrial damage after oxidative stress in HT-22 neurons and shows similar effects as obtained with AIF silencing. Although AIF itself is not a part of complex I, a role of AIF in the biogenesis and/or maintenance of this polyprotein complex is already postulated [13]. Our findings of slightly decreased AIF expression levels after rotenone-treatment confirm this and suggest a mutual stabilization of AIF and complex I thereby regulating neuronal survival towards oxidative stress. The fact that high doses of the complex I inhibitor rotenone lead to lethal stress is in accordance with a common link of AIF and mitochondrial complex I since mice, completely depleted in AIF, are

**Fig. 8** Low doses of rotenone prevent mitochondrial integrity and function. **a** Fluorescence photomicrographs show that rotenone (20 nM) prevents the fission of mitochondria in glutamate-exposed (3 mM, 14 h) HT-22 cells. Cells were stained with Mitotracker red 30 min before glutamate and rotenone treatment. Bar scale 20  $\mu$ m. **b** Quantification of mitochondrial morphology: Category I (*Cat I*): fused, Category II (*Cat II*): intermediate, Category III (*Cat III*): fragmented mitochondria; at least 500 cells were counted per condition blinded to treatment conditions. Values are given from four independent experiments (<sup>###</sup> $p < 0.01$  compared to category I glutamate treated control; \* $p < 0.05$  compared to category III glutamate treated control). **c** Lipid peroxides were measured by Bodipy FACS analysis 13 h following glutamate (glut) treatment (2 and 3 mM). Values are given from three independent experiments; \*\*\* $p < 0.001$  compared to glutamate treated control cells (2 mM); <sup>###</sup> $p < 0.001$  compared to glutamate treated control cells (3 mM). **d** Rotenone receiving cells (20 nM) were preserved from loss in ATP levels 14 h after glutamate treatment (3 mM).  $N = 8$ ; \*\*\* $p < 0.001$  compared to control cells. All statistics were obtained using ANOVA, Scheffé test

also no longer viable [11, 32]. Complex I is part of a complex I/III/IV supercomplex (the so-called respirasome) [33], and consists of 46 protein subunits from which seven are encoded by the mitochondrial genome. The remaining subunits are encoded in the nucleus, translated in the cytosol and imported into the mitochondria [34]. Biochemical analyses suggest that the complex I depletion in AIF-deficient cells derive from reduced expression of several of these nuclear encoded subunits [13]. On the mRNA level there are controversial studies reporting that neither AIF depletion nor deletion has major effects on the expression levels of respiratory chain subunits [13]. However, another study reports a partial reduction on mRNA levels of respiratory chain subunits [35]. Thus, AIF may regulate complex I levels by post-transcriptional mechanisms. Furthermore, there are contrary systematic proteomic studies, some of these suggesting that AIF is an integral part of the respiratory chain complexes [13, 36]. Further investigations are needed to determine how AIF is involved in the stability or the assembly of complex I and why this stabilization is mutual, i.e. affects also AIF stability.

Our findings that mitochondria are fully preserved in both models of protection, i.e. AIF depletion and low dose rotenone, demonstrate that neuroprotection mediated by AIF deficiency is not just attributed to reduced amounts of AIF available for translocation into the nucleus but it postulates a preconditioning effect upstream of AIF release from the mitochondria. The reduced complex I expression levels and the slightly decreased MMP in AIF-depleted cells under standard culture conditions further support this hypothesis and indicate changes of the respiratory chain as an underlying mechanism.

It is already known that inhibition of the respiratory chain can induce tolerance to e.g. focal cerebral ischemia [16]. Since AIF plays a major role in intrinsic pathways of caspase-independent neuronal death in model systems of





cerebral ischemia [3–5, 27] a preconditioning effect mediated by complex I inhibition is perfectly feasible. However, persistent downregulation of AIF in Hq mice results in progressing ataxia, blindness, growth retardation and weight loss in the animals [28]. Pathogenetic AIF mutation in humans causes muscular atrophy, neurological and psychomotor abnormalities and progressive mitochondrial encephalomyopathy [37]. Since there are no tools available that can selectively target the proapoptotic function of AIF or that can downregulate AIF for a short time, AIF is not a recommended direct target for the therapy of cerebral ischemia or traumatic brain injury, to date. Rather, mechanisms of AIF release upstream of mitochondrial damage are suggested as potential targets for therapeutic strategies.

Preconditioning effects are often described to promote a small decrease in the efficiency of NADH oxidation by the respiratory chain, which increases mitochondrial ROS release followed by activation of  $\text{mitoK}_{\text{ATP}}$  channels [38–42]. However, we could not detect increased lipid peroxide levels in AIF siRNA transfected cells suggesting that increased ROS production in AIF-depleted cells was not the major mechanism of the preconditioning effect. This is in line with previous studies showing that ROS production under basal conditions or stimulated by complex I inhibitors were not different in mitochondria from Hq mouse brain compared to wild type mitochondria [12]. These results suggest that AIF does not directly modulate ROS production in mitochondria. Thus, other mechanisms linked to reduced complex I activity seem to be responsible for the preconditioning effect of AIF depletion, such as, for example, the observed slight mitochondrial membrane depolarization.

Collectively, our results favor the hypothesis that AIF depletion is linked to a decrease in complex I expression levels and respiratory chain activity. These preconditioning effects lead to a stabilization of mitochondria and thus to delayed cell death after the glutamate challenge and related induction of oxidative stress. Therefore, our data demonstrate an essential association between AIF and the mitochondrial respiratory chain in modulating each other's stability thereby determining neuronal survival in paradigms of detrimental oxidative stress.

## Materials and methods

### Cells

HT-22 cells were cultured in Dulbecco's modified Eagle medium (DMEM, Invitrogen, Karlsruhe, Germany) supplemented with 10 % heat-inactivated fetal calf serum, 100 U/ml penicillin, 100 mg/ml streptomycin and 2 mM glutamine (all Sigma-Aldrich, Munich, Germany). For

inducing apoptosis, glutamate (2–5 mM) was added to the medium for 11–15 h.

siRNA transfections were performed in 24-well plates. For each well 1.2  $\mu\text{l}$  Lipofectamine RNAiMax (Invitrogen) was mixed with siRNA and filled up to 100  $\mu\text{l}$  with Opti-mem I (Invitrogen). Afterwards, an antibiotic free cell suspension (33,333 cells/well) was added. After 48 h cells were treated in the 24-well plate or seeded into another culturing format depending on the type of experiment. Following siRNA sequences synthesized by Eurofins MWG Operon (Ebersberg, Germany) were used: AAGAG AAACAGAGAAGAGCCA (AIF siRNA 1), AUGUCAC AAAGACACUGCA (AIF siRNA 2) and AAGAGAAA AAGCGAAGAGCCA (negative control). Gene silencing was verified by RT-PCR and Western Blotting.

Rotenone (Sigma-Aldrich) was applied in combination with glutamate or as pretreatment (9 h) followed by a washout and subsequent glutamate treatment. The final concentration of rotenone was 20 nM. DMSO (Sigma-Aldrich) was used as a standard solvent with a maximum concentration of  $2 \times 10^{-3}$  % in all experiments.

### Viability assays

Quantification of cell viability was performed in 96-well plates by MTT (3-(4,5-dimethylthiazol-2-yl)-2,5-diphenyltetrazolium bromide) reduction at 0.25 mg/ml for 1 h. Absorbance was determined after dissolving the MTT dye in DMSO at 570 versus 630 nm (FluoStar, BMG Labtech, Offenburg, Germany). In addition, real-time detection of cellular viability was performed by cellular impedance measurements using the xCELLigence system (Roche, Penzberg, Germany) as previously described [21].

### Lipid peroxidation

For detection of cellular lipid peroxidation, cells were loaded with 2 mM BODIPY 581/591 C11 (Invitrogen) in standard medium at indicated time points. Cells were collected, washed and resuspended in PBS. The flow cytometry was performed using 488 nm UV line argon laser for excitation and BODIPY emission was recorded at 530 and 585 nm. Data were collected from at least 10,000 cells. Measurements are representative of at least three independent experiments.

### Mitochondrial transmembrane potential measurements

Changes of the MMP ( $\Delta\Psi_{\text{m}}$ ) were detected by DIOC6(3) fluorescence-based assay and TMRE assay. Isolated 25–50  $\mu\text{g}$  mitochondria were incubated with 20 nM DIOC6(3) dye. As a positive control for a complete loss of  $\Delta\Psi_{\text{m}}$ , CCCP (50  $\mu\text{M}$ ) protonophore was applied on intact

mitochondria.  $\Delta\Psi_m$  was analyzed by a FLUOstar Optima fluorescence plate reader. Measurements were performed in triplicate and are representative of at least three independent experiments.

For detection of  $\Delta\Psi_m$  in whole cells, the MitoPT™ TMRE kit (Immunochemistry Technologies, Hamburg, Germany) was used. The cells were incubated for 20 min at 37 °C with TMRE (tetramethylrhodamin ethyl ester) after glutamate treatment. Cells were collected, washed with PBS and resuspended in assay buffer. Flow cytometry was performed using emission at 680 nm. Data were collected from at least 10,000 cells from at least four independent experiments.

### Mitochondrial morphology

For analysis of the mitochondrial morphology cells were stained with MitoTracker (Invitrogen) and nuclei were counterstained with DAPI (4',6-diamidino-2-phenylindole dihydrochloride) before the glutamate treatment. At indicated time points cells were fixed with 4 % paraformaldehyde (PFA). At least 500 cells per condition were counted blind to treatment conditions in at least four independent experiments. Images were acquired using a fluorescence microscope (Leica, Wetzlar, Germany). Pictures were taken using confocal microscopy at 633 nm with a LP650 filter (Zeiss, Oberkochen, Germany).

### ATP measurement

Transfected HT-22 neurons were seeded in white 96-well plates (Greiner Bio one, Frickenhausen, Germany) for luminescence measurements. ATP levels were detected at indicated time points by detection of luminescence using the ViaLight MDA Plus-Kit (Lonza, Verviers, Belgium). The cells were treated with nucleotide releasing reagent and ATP monitoring reagent was injected into each well. Luminescence was detected immediately (FluoStar, BMG Labtech, Offenburg, Germany). The values are given as relative values in % to control.

### Protein analysis

For obtaining total cell protein extracts HT-22 cells were seeded in 24-well plates (Greiner Bio one). Cells were washed with PBS and lysed with buffer containing Mannitol 0.25 M, Tris 0.05 M, EDTA 1 M, EGTA 1 M, DTT 1 mM, Triton-X 1 % (all Sigma-Aldrich), supplemented with Complete Mini Protease Inhibitor Cocktail (Roche). To remove insoluble membrane fragments, extracts were centrifuged at 13,000×g for 15 min at 4 °C.

For mitochondrial enriched extracts cells were lysed in a buffer containing 250 mM sucrose (Merck, Darmstadt, Germany), 20 mM HEPES (Sigma-Aldrich), 3 mM EDTA supplemented with Complete Mini Protease Inhibitor Cocktail (pH 7.5). Cells were disrupted using a glass douncer followed by 15 passes with a 20G needle. After centrifugation at 900×g for 10 min supernatant was collected and the pellet was disrupted a second time. The supernatant was centrifuged at 16,800×g for 10 min and the resulting pellet was re-suspended in fresh buffer.

Western Blot analysis was performed as previously described [3]. Briefly, the blot was probed with an anti-AIF goat polyclonal antibody (Santa Cruz, Biotechnology, Santa Cruz, CA, USA), anti-TIM 23 (BD Biosciences, Heidelberg, Germany), anti-actin (MB Biomedicals, Illkirch Cedex, France) or Mitoprofile antibody (Abcam, Cambridge, UK) at 4 °C overnight. Membranes were then exposed to the appropriate HRP-conjugated secondary antibody (Vector Laboratories, Burlingame, CA, USA), followed by a chemiluminescence detection of antibody binding. Chemidoc software (Bio-Rad, Munich, Germany) was used for detection of Western Blot signals.

### RT-PCR

Total RNA was extracted from cells (Nucleospin RNA II kit, Macherey–Nagel, Düren, Germany) 72 h after transfection. Primers for AIF were: forward, 5'-GCGTAATACGACTC ACTATAGGGAGATCCAGGC AACTTGTTCAGC-3', and reverse, 5'-GCGTAATACGACTCACTATAGGGA GACCTCTGCTCCAGCCC TATCG-3'. Primers for glyceraldehyde-3-phosphate dehydrogenase (GAPDH) were: forward, 5'-AGGCCGGTGCTGAGTAT-3', and reverse, 5'-TGCCTGCTTACCACCTTCT-3' (all Eurofins MWG Operon). RT-PCR for AIF and GAPDH was performed with SuperScript III One-Step RT-PCR kit with Platinum Taq (Invitrogen) as follows: initial denaturation at 95 °C for 2 min; amplification by 28–30 cycles of 30 s 95 °C, 1 min 57 °C, and 2 min 70 °C; and final extension at 70 °C for 10 min. RT-PCR products were visualized under UV illumination after electrophoresis on a 1.5 % agarose gel.

### Statistical analysis

All data are given as mean ± standard deviation (S.D.). For statistical comparisons between treatment groups analysis of variance (ANOVA) was performed followed by Scheffé's post hoc test. Calculations were performed with the Winstat standard statistical software package.

**Acknowledgments** We thank the excellent technical support by Mrs. Renate Hartmannsgruber and Mrs. Katharina Elsässer. Furthermore, we thank Mrs. Emma Esser for careful editing of the manuscript

and Mr. Alexander Seiler (Roche Diagnostics GmbH) for providing support with the xCELLigence system.

**Conflict of interests** The authors have declared that no conflict of interests exist.

## References

- Susin SA, Lorenzo HK, Zamzami N et al (1999) Molecular characterization of mitochondrial apoptosis-inducing factor. *Nature* 397:441–446
- Susin SA, Zamzami N, Castedo M et al (1996) Bcl-2 inhibits the mitochondrial release of an apoptogenic protease. *J Exp Med* 184:1331–1341
- Plesnila N, Zhu C, Culmsee C et al (2004) Nuclear translocation of apoptosis-inducing factor after focal cerebral ischemia. *J Cereb Blood Flow Metab* 24:458–466
- Culmsee C, Zhu C, Landshamer S et al (2005) Apoptosis-inducing factor triggered by poly(ADP-ribose) polymerase and Bid mediates neuronal cell death after oxygen-glucose deprivation and focal cerebral ischemia. *J Neurosci* 25:10262–10272
- Zhu C, Qiu L, Wang X et al (2003) Involvement of apoptosis-inducing factor in neuronal death after hypoxia-ischemia in the neonatal rat brain. *J Neurochem* 86:306–317
- Slemmer JE, Zhu C, Landshamer S et al (2008) Causal role of apoptosis-inducing factor for neuronal cell death following traumatic brain injury. *Am J Pathol* 173:1795–1805
- Cheung EC, Melanson-Drapeau L, Cregan SP et al (2005) Apoptosis-inducing factor is a key factor in neuronal cell death propagated by BAX-dependent and BAX-independent mechanisms. *J Neurosci* 25:1324–1334
- Delavallee L, Cabon L, Galan-Malo P et al (2011) AIF-mediated caspase-independent necroptosis: a new chance for targeted therapeutics. *IUBMB Life* 63:221–232
- Tretter L, Sipos I, dam-Vizi V (2004) Initiation of neuronal damage by complex I deficiency and oxidative stress in Parkinson's disease. *Neurochem Res* 29:569–577
- Landshamer S, Hoehn M, Barth N et al (2008) Bid-induced release of AIF from mitochondria causes immediate neuronal cell death. *Cell Death Differ* 15:1553–1563
- Joza N, Susin SA, Dugas E et al (2001) Essential role of the mitochondrial apoptosis-inducing factor in programmed cell death. *Nature* 410:549–554
- Chinta SJ, Rane A, Yadava N et al (2009) Reactive oxygen species regulation by AIF- and complex I-depleted brain mitochondria. *Free Radic Biol Med* 46:939–947
- Vahsen N, Cande C, Briere JJ et al (2004) AIF deficiency compromises oxidative phosphorylation. *EMBO J* 23:4679–4689
- Cheung EC, Joza N, Steenaart NA et al (2006) Dissociating the dual roles of apoptosis-inducing factor in maintaining mitochondrial structure and apoptosis. *EMBO J* 25:4061–4073
- Joza N, Oudit GY, Brown D et al (2005) Muscle-specific loss of apoptosis-inducing factor leads to mitochondrial dysfunction, skeletal muscle atrophy, and dilated cardiomyopathy. *Mol Cell Biol* 25:10261–10272
- Wiegand F, Liao W, Busch C et al (1999) Respiratory chain inhibition induces tolerance to focal cerebral ischemia. *J Cereb Blood Flow Metab* 19:1229–1237
- Bannai S (1986) Exchange of cystine and glutamate across plasma membrane of human fibroblasts. *J Biol Chem* 261:2256–2263
- Grohm J, Plesnila N, Culmsee C (2010) Bid mediates fission, membrane permeabilization and peri-nuclear accumulation of mitochondria as a prerequisite for oxidative neuronal cell death. *Brain Behav Immun* 24:831–838
- Grohm J, S.W.Kim, U.Mamrak et al. (2012) Inhibition of Drp1 provides neuroprotection in vitro and in vivo. *Cell Death Differ*. doi:10.1038/cdd.2012.18
- Tobaben S, Grohm J, Seiler A et al (2011) Bid-mediated mitochondrial damage is a key mechanism in glutamate-induced oxidative stress and AIF-dependent cell death in immortalized HT-22 hippocampal neurons. *Cell Death Differ* 18:282–292
- Diemert S, Dolga AM, Tobaben S et al (2012) Impedance measurement for real time detection of neuronal cell death. *J Neurosci Methods* 203:69–77
- Cregan SP, Fortin A, MacLaurin JG et al (2002) Apoptosis-inducing factor is involved in the regulation of caspase-independent neuronal cell death. *J Cell Biol* 158:507–517
- Polster BM, Basanez G, Etxebarria A et al (2005) Calpain I induces cleavage and release of apoptosis-inducing factor from isolated mitochondria. *J Biol Chem* 280:6447–6454
- Wang Y, Dawson VL, Dawson TM (2009) Poly(ADP-ribose) signals to mitochondrial AIF: a key event in parthanatos. *Exp Neurol* 218:193–202
- Wang Y, Kim NS, Haince JF et al (2011) Poly(ADP-ribose) (PAR) binding to apoptosis-inducing factor is critical for PAR polymerase-1-dependent cell death (parthanatos). *Sci Signal* 4:ra20
- Yu SW, Wang H, Poitras MF et al (2002) Mediation of poly(-ADP-ribose) polymerase-1-dependent cell death by apoptosis-inducing factor. *Science* 297:259–263
- Zhu C, Wang X, Huang Z et al (2007) Apoptosis-inducing factor is a major contributor to neuronal loss induced by neonatal cerebral hypoxia-ischemia. *Cell Death Differ* 14:775–784
- Klein JA, Longo-Guess CM, Rossmann MP et al (2002) The harlequin mouse mutation downregulates apoptosis-inducing factor. *Nature* 419:367–374
- Daugas E, Susin SA, Zamzami N et al (2000) Mitochondrial-nuclear translocation of AIF in apoptosis and necrosis. *FASEB J* 14:729–739
- Osato K, Sato Y, Ochiishi T et al (2010) Apoptosis-inducing factor deficiency decreases the proliferation rate and protects the subventricular zone against ionizing radiation. *Cell Death Dis* 1:e84
- Benit P, Goncalves S, Dassa EP et al (2008) The variability of the harlequin mouse phenotype resembles that of human mitochondrial-complex I-deficiency syndromes. *PLoS ONE* 3:e3208
- Brown D, Yu BD, Joza N et al (2006) Loss of Aif function causes cell death in the mouse embryo, but the temporal progression of patterning is normal. *Proc Natl Acad Sci USA* 103:9918–9923
- Schagger H (2001) Respiratory chain supercomplexes. *IUBMB Life* 52:119–128
- Dimauro S, Rustin P (2009) A critical approach to the therapy of mitochondrial respiratory chain and oxidative phosphorylation diseases. *Biochim Biophys Acta* 1792:1159–1167
- Pospisilik JA, Knauf C, Joza N et al (2007) Targeted deletion of AIF decreases mitochondrial oxidative phosphorylation and protects from obesity and diabetes. *Cell* 131:476–491
- Schilling B, Murray J, Yoo CB et al (2006) Proteomic analysis of succinate dehydrogenase and ubiquinol-cytochrome c reductase (Complex II and III) isolated by immunoprecipitation from bovine and mouse heart mitochondria. *Biochim Biophys Acta* 1762:213–222
- Modjtahedi N, Giordanetto F, Kroemer G (2010) A human mitochondriopathy caused by AIF mutation. *Cell Death Differ* 17:1525–1528
- Busija DW, Gaspar T, Domoki F et al (2008) Mitochondrial-mediated suppression of ROS production upon exposure of neurons to lethal stress: mitochondrial targeted preconditioning. *Adv Drug Deliv Rev* 60:1471–1477

39. Dirnagl U, Meisel A (2008) Endogenous neuroprotection: mitochondria as gateways to cerebral preconditioning? *Neuropharmacology* 55:334–344
40. Jou MJ (2008) Pathophysiological and pharmacological implications of mitochondria-targeted reactive oxygen species generation in astrocytes. *Adv Drug Deliv Rev* 60:1512–1526
41. Ravati A, Ahlemeyer B, Becker A, Kriegstein J (2000) Preconditioning-induced neuroprotection is mediated by reactive oxygen species. *Brain Res* 866:23–32
42. Ravati A, Ahlemeyer B, Becker A et al (2001) Preconditioning-induced neuroprotection is mediated by reactive oxygen species and activation of the transcription factor nuclear factor-kappaB. *J Neurochem* 78:909–919